

This work was written as part of one of the author's official duties as an Employee of the United States Government and is therefore a work of the United States Government. In accordance with 17 U.S.C. 105, no copyright protection is available for such works under U.S. Law.

Public Domain Mark 1.0

<https://creativecommons.org/publicdomain/mark/1.0/>

Access to this work was provided by the University of Maryland, Baltimore County (UMBC) ScholarWorks@UMBC digital repository on the Maryland Shared Open Access (MD-SOAR) platform.

Please provide feedback

Please support the ScholarWorks@UMBC repository by emailing scholarworks-group@umbc.edu and telling us what having access to this work means to you and why it's important to you. Thank you.

Comparison of columnar water-vapor measurements from solar transmittance methods

Beat Schmid, Joseph J. Michalsky, Donald W. Slater, James C. Barnard, Rangasayi N. Halthore, James C. Liljegren, Brent N. Holben, Thomas F. Eck, John M. Livingston, Philip B. Russell, Thomas Ingold, and Ilya Slutsker

In the fall of 1997 the Atmospheric Radiation Measurement program conducted a study of water-vapor-abundance-measurement at its southern Great Plains site. The large number of instruments included four solar radiometers to measure the columnar water vapor (CWV) by measuring solar transmittance in the 0.94- μm water-vapor absorption band. At first, no attempt was made to standardize our procedures to the same radiative transfer model and its underlying water-vapor spectroscopy. In the second round of comparison we used the same line-by-line code (which includes recently corrected H_2O spectroscopy) to retrieve CWV from all four solar radiometers, thus decreasing the mean CWV by 8–13%. The remaining spread of 8% is an indication of the other-than-model uncertainties involved in the retrieval.

© 2001 Optical Society of America

OCIS codes: 010.0010, 010.1110, 010.1320, 010.7340.

1. Introduction

Solar transmittance methods can provide water-vapor abundance values from direct or reflected sunlight measurements in spectral channels in and adjacent to water-vapor absorption bands. The water-vapor transmittance thus derived has to be translated into columnar water vapor (CWV). Although this relationship is well known qualitatively,¹ it has proved difficult to quantify. Attempts to do so for water-vapor absorption bands in the near infrared date back to 1912.² But even in the past decade there has been a steady stream of publications on this subject. For example, results from ground-based retrievals of CWV from solar radiometers have been reported widely (see Ingold *et al.*³ and references therein). Recently, Schmid *et al.*⁴ reported on CWV retrievals with an airborne sunphotometer. Instruments aboard satellites, such as the Stratospheric Aerosol and Gas Experiment (SAGE II) and the Polar ozone and aerosol measurements (POAM II and POAM III) use the solar occultation technique (i.e., measuring the solar transmittance through the limb of the atmosphere) to retrieve water vapor.^{5,6} Fi-

nally, CWV is also retrieved from airborne instruments [such as the Airborne Visible Infrared Imaging Spectrometer (AVIRIS)] and spaceborne instruments [such as the Polarization and Directionality of the Earth's Reflectance (POLDER) and the Moderate-Resolution Imaging Spectroradiometer (MODIS)] that measure the solar radiance reflected by the Earth's surface.^{7–10}

Recent findings that the H_2O line intensities in the visible and near-infrared portions of the widely used HITRAN96 database¹¹ were in error¹² and that H_2O lines (especially weak ones) might be missing from the current databases^{13,14} have stimulated renewed discussion of the accurate conversion of measured water-vapor transmittance into amounts of water vapor.

In the fall of 1997 the Atmospheric Radiation Measurement (ARM) program¹⁵ conducted the second intensive observation period (IOP) to study water vapor at its southern Great Plains (SGP) site. The large number of instruments present, such as radiosondes, microwave radiometers, Raman lidars, global positioning system receivers, and infrared spectrometers included four solar radiometers to measure water vapor.¹⁶

In this paper we focus on the four solar radiometers that retrieve CWV by measuring solar transmittance in the 0.94- μm water-vapor absorption band. The measurements were made from 15 September to 5 October 1997 at the SGP ARM central facility near

The authors' affiliations are listed in Appendix A.

Received 12 June 2000; revised manuscript received 16 January 2001.

0003-6935/01/01886-11\$15.00/0

© 2001 Optical Society of America

Lamont, Oklahoma (36° 36' N, 97° 29' W; 316 m above sea level). Dry to highly humid conditions, with CWV ranging from 1 to 5 cm, were experienced over the three-week period. As one of the steps in the CWV retrievals the aerosol component must be subtracted from the total transmittance in the 0.94- μm band. A comparison of aerosol optical depth (AOD) among the same four radiometers was presented previously.¹⁷

Following the philosophy of the AOD comparison just mentioned, we first made no attempt to equal our procedures used to derive CWV from the four radiometers. We found that three methods had been used in conjunction with three radiative transfer models. In a second round we used the same radiative transfer model (with its underlying spectroscopy corrected according to Giver *et al.*¹²) for all instruments. In this paper we show the results from both rounds.

2. Instrumentation

The NASA Ames Research Center deployed its six-channel Ames Airborne Tracking Sunphotometer (AATS-6) at the SGP central facility of the ARM for this IOP. The instrument was operated on the ground. The AATS-6, described by Matsumoto *et al.*,¹⁸ uses an active Sun sensor to keep the instrument pointed at the solar disk. The central wavelengths and FWHM for the filters are listed in Table 1. The Si detectors are held at a constant temperature of 45 ± 0.6 °C. The field of view FOV of the AATS-6 is 4.5°. A measurement sequence consists of an average of nine scans over all six channels (and housekeeping data) taken within 3 s. This sequence was repeated at 12-s intervals.

At the ARM SGP central facility a Cimel Sun-sky photometer measures AOD and CWV. This instrument is also part of AERONET, a worldwide network of Cimel sunphotometers.¹⁹ The Cimel CE-318 instrument points to the Sun based on an ephemeris calculation and then fine tunes the pointing with an active Sun-sensor adjustment. Samples consist of triplets of measurements in which each of the second and the third members of the triplets begins 30 s later than the previous one and consists of eight filter measurements completed within 8 s; the triplets are repeated at every quarter air mass from two to seven air masses and every 15 mins; when there are fewer than two air masses. The central wavelength and the FWHM for each filter are listed in Table 1. The FOV is 1.2°. The temperature of the instrument is monitored but not controlled.

A multifilter rotating shadow-band radiometer²⁰ (MFRSR) has a hemispherical FOV. A band is positioned to move alternately completely out of the FOV and then to block the Sun according to a calculation of solar hour angle, permitting a measurement of the total downward and diffuse-downward irradiance. The difference between the two measurements is the direct solar component normal to the receiver and the direct normal component is calculated by dividing by the cosine of the solar-zenith

Table 1. Central Wavelengths (λ) and Bandwidths ($\Delta\lambda$, FWHM) of Filtered Instruments

| AATS-6 | | Cimel | | MFRSR | |
|----------------|----------------------|----------------|----------------------|----------------|----------------------|
| λ (nm) | $\Delta\lambda$ (nm) | λ (nm) | $\Delta\lambda$ (nm) | λ (nm) | $\Delta\lambda$ (nm) |
| 380.1 | 5.0 | 340 | 2 | 413.9 | 10 |
| | | 380 | 4 | | |
| 450.7 | 5.1 | 440 | 10 | 499.3 | 10 |
| 525.3 | 5.0 | 500 | 10 | | |
| 863.9 | 5.3 | 670 | 10 | 608.5 | 10 |
| | | 870 | 10 | 665.1 | 10 |
| | | 940 | 10 | 859.9 | 10 |
| | | 940 | 10 | 938.0 | 10 |
| 1020.7 | 5.0 | 1020 | 10 | | |

angle and correcting for the angular response of the quasi-Lambertian detector. Sampling occurs at 20-s intervals. The central wavelength and the FWHM for each filter are given in Table 1. The temperature is held at 40 ± 2 °C.

The rotating shadow-band spectroradiometer²¹ (RSS) has a Lambertian receiver and a shadowing sequence similar to those of the MFRSR; however, the detector is a 512-element photodiode array that receives its light input from the focus of a prism spectrograph. Sampling is performed once each minute. The spectral resolution from 350 to 1050 nm diminishes from 0.3 to 8 nm because of the prism dispersive element. The temperature is held at 40 ± 2 °C.

In what follows, we refer to all four instruments as solar radiometers.

3. Methodology

In the derivation of atmospheric transmittance, we distinguish between atmospheric window channels and gaseous-absorption channels. The window channels are located outside molecular absorption bands such as O₂ and H₂O and are normally used for determining AOD.

A. Aerosol Optical Depth

For atmospheric window channels the instrument output voltage $V(\lambda)$, obtained when the directly transmitted solar irradiance is observed over a small band-pass $\Delta\lambda$ centered at wavelength λ , can be described by the Beer–Lambert–Bouguer attenuation law:

$$V(\lambda) = V_0(\lambda)d^{-2} \exp[-m\tau(\lambda)], \quad (1)$$

where $V_0(\lambda)$ is the instrument calibration constant, d is the Earth–Sun distance (in astronomical units) at the time of observation, $\tau(\lambda)$ is the spectral optical depth, and m is the relative optical air mass, a function of the solar zenith angle.²² Taking the logarithm of Eq. (1) leads to

$$\ln V(\lambda) = \ln[V_0(\lambda)d^{-2}] - m\tau(\lambda). \quad (2)$$

If a series of measurements is taken over a range of air masses m during which the optical depth $\tau(\lambda)$

remains constant, $V_0(\lambda)$ can be determined from the ordinate intercept of a least-squares fit when the left-hand side of Eq. (2) is plotted versus m . This procedure is commonly known as the Langley-plot calibration.

In Eq. (1) several attenuators contribute to $\tau(\lambda)$:

$$\tau(\lambda) = \tau_R(\lambda) + \tau_3(\lambda) + \tau_2(\lambda) + \tau_a(\lambda), \quad (3)$$

where the subscripts R , 3, 2, and a refer to Rayleigh scattering by air molecules, absorption owing to O_3 and NO_2 , and attenuation caused by aerosol particles, respectively.

A refined Langley technique,^{23–25} which uses an individual air-mass expressions for each attenuator in Eq. (3), was used for the AATS-6 but not for the other three instruments. We calibrated the window channels of the AATS-6 by averaging the results of six successful morning Langley plots performed at the Mauna Loa Observatory (MLO) in Hawaii (19° 32' N, 155° 34' W; 3397 m above sea level) approximately two weeks before the IOP. Because of its high altitude, which results in nighttime downslope winds, and its large distance from significant pollution sources, the MLO is a prime site for performing morning Langley plots.

Calibration of Cimel #27 (the instrument deployed at the SGP during the IOP) is based on a transfer of the calibration from Cimel #37, the reference instrument. The intercalibrations were performed at Goddard Space Flight Center in Maryland on 30 August 1997 and 3 November 1997 at midday for a period of 1–2 h. The reference instrument itself was calibrated by the Langley technique at the MLO in May and September 1997.

Calibration of the MFRSR and the RSS was based on a robust estimate from the 20 nearest successful Langley plots at the SGP. One of those 20 nearest successful Langley plots was obtained with data from the morning of 29 September 1997. A Langley plot performed with the AATS-6 during the same morning yielded calibration constants that agreed to within 0.5% with the MLO results obtained two weeks before the IOP. This result suggests that during this particular morning the atmosphere over the SGP was sufficiently stable to yield unbiased Langley-plot results to be used in the robust estimate of the calibration constants for the MFRSR and the RSS.

Once the calibration constants $V_0(\lambda)$ of the window channels are known, the AOD $\tau_a(\lambda)$ can be determined from Eqs. (2) and (3). The AOD's obtained from each instrument were derived independently of one another. Although the methods to remove Rayleigh, O_3 , and NO_2 optical depths coincide in some instances, there was no attempt to make a uniform reduction to AOD from the total optical depth. Nevertheless, AOD's ($\lambda = 380$ – 1020 nm) obtained during the IOP by the Cimel, MFRSR, and RSS instruments agreed with AATS-6 values to within 0.025 (rms). The AOD's in atmospheric windows adjacent to the $0.94\text{-}\mu\text{m}$ band agreed to within 0.015 (rms).¹⁷

B. Columnar Water Vapor

The Beer–Lambert–Bouguer law, which is monochromatic in nature, can be applied over small bandpasses $\Delta\lambda$ with negligible error as long as the spectral variation of transmittance inside the bandpass is small. In regions of strong spectral variation of molecular absorption, such as the near-infrared water-vapor absorption bands, Eq. (1) can be expressed as²⁶

$$V(\lambda) = V_0(\lambda)d^{-2} \exp\{-m[\tau_R(\lambda) + \tau_a(\lambda) + \tau_3(\lambda)]\}T_w(\bar{\lambda}). \quad (4)$$

(Note that there is no absorption that is due to NO_2 in the water-vapor absorption channels used here.) $T_w(\bar{\lambda})$ is the band- and source-weighted water-vapor transmittance:

$$T_w(\bar{\lambda}) = \frac{\int_{\Delta\lambda} E_0(\lambda)S(\lambda)\exp[-m\tau_w(\lambda)]d\lambda}{\int_{\Delta\lambda} E_0(\lambda)S(\lambda)d\lambda}, \quad (5)$$

where $\tau_w(\lambda)$ is the strongly varying water-vapor absorption optical depth, $E_0(\lambda)$ is the exoatmospheric solar irradiance, and $S(\lambda)$ is the instrument response. It should be noted that, even if $E_0(\lambda)$ and $S(\lambda)$ were effectively constant over $\Delta\lambda$, the strong spectral variation of $\tau_w(\lambda)$ would be sufficient to require the band-weighted transmittance $T_w(\bar{\lambda})$ in Eq. (4). Also, Eq. (4) does not follow the Beer–Lambert–Bouguer law, as $T_w(\bar{\lambda})$ generally cannot be modeled by an exponential with a negative argument of air mass times a constant band-weighted optical depth. Hence, for channels in strong absorption bands, $V_0(\lambda)$ can no longer be found by use of the traditional or the refined Langley method. In this section we discuss three approaches to determining $V_0(\lambda)$ and $T_w(\bar{\lambda})$ to retrieve CWV from measurements in the $0.94\text{-}\mu\text{m}$ water-vapor absorption band.

1. Method A: Modified Langley-Plot Technique

If $T_w(\bar{\lambda})$ can be modeled by an exponential with a negative argument proportional to some power of the slant-path absorber amount, such as

$$T_w(\bar{\lambda}) = \exp[-a(mu)^b], \quad (6)$$

where u is the columnar water vapor and a and b are constants, then $V_0(\lambda)$ can be determined by use of a modified Langley-plot technique: Substituting Eq. (6) into Eq. (4), rearranging the terms, and taking the logarithm lead to

$$\ln V(\lambda) + m[\tau_a(\lambda) + \tau_R(\lambda) + \tau_3(\lambda)] = \ln[V_0(\lambda)d^{-2}] - a(mu)^b. \quad (7)$$

We now construct modified Langley plots by plotting the left-hand side of Eq. (7) versus m^b . Therefore the instantaneous values of the AOD $\tau_a(\lambda)$ in the water-vapor absorption channel must be known. These are estimated from the solar radiometer's win-

dow wavelengths by use of a quadratic fit on a log–log scale of $\tau_a(\lambda)$ versus λ . This requires that the $V_0(\lambda)$ values of the window channels be determined before modified Langley plots are constructed. It is evident that for the construction of modified Langley plots the columnar water-vapor amount should remain constant, at least for the 1.5–2-h period of Langley data acquisition.

$T_w(\bar{\lambda})$ is typically computed according to Eq. (5) with a radiative transfer model over a range of slant-path water-vapor amounts. Constants a and b in Eq. (6) are then found by a curve-fitting procedure.^{3,27–29} Combining Eqs. (4) and (6) yields a CWV of

$$u = \frac{1}{m} \left\{ \frac{1}{a} \left[\ln \frac{V_0(\lambda)d^{-2}}{V(\lambda)} - m[\tau_R(\lambda) + \tau_a(\lambda) + \tau_3(\lambda)] \right] \right\}^{1/b}. \quad (8)$$

For the research reported in this paper we used method A to obtain CWV for the AATS-6 and the Cimel instruments. For the Cimel instrument the standard AERONET algorithm was used: we used the same typical filter function [$S(\lambda)$ in Eq. (5)] for all the instruments in the network in conjunction with LOWTRAN 7 computations³⁰ to determine one set of a and b . The 940-nm channel of reference instrument Cimel #37 was calibrated by the modified Langley technique at the MLO in May and September 1997. For both calibration periods the $V_0(\lambda)$ values of four morning modified Langley plots were averaged. The relative standard deviations in $V_0(\lambda)$ were $\sim 2\%$.

For the AATS-6 we used the MODTRAN 3.5 v1.1 program³⁰ to determine one set of a and b values for the MLO and several sets (covering different ranges of $m_w u$) for SGP conditions. For $S(\lambda)$ in Fig. (5) we used the filter function of the 941.4-nm channel as measured by the manufacturer (Barr Associates, Inc., Westford, Mass.) in February 1994. We determined the $V_0(\lambda)$ value of that channel by averaging the results of five morning modified Langley plots (standard deviation, 1.2%) performed at the MLO two weeks before the IOP.

2. Method B: Differential Lamp–Solar Spectrum Technique

The differential lamp–solar spectrum method has been described in detail by Michalsky *et al.*³¹ Only a brief summary is given here. Method B avoids the need to calibrate by the modified Langley method. Instead, it requires values of the instrument output $V_L(\lambda)$ when a calibration lamp is viewed, and the lamp irradiance $E_L(\lambda)$ and the extraterrestrial solar spectrum $E_0(\lambda)$, both convolved with filter function $S(\lambda)$. To retrieve CWV we consider the ratio of the

radiometer output voltages measured in channels in (λ_{in}) and adjacent to (λ_{out}) the 0.94- μm band:

$$\frac{V(\lambda_{in})}{V(\lambda_{out})} = \frac{E_0(\lambda_{in})E_L(\lambda_{out})V_L(\lambda_{in})}{E_0(\lambda_{out})E_L(\lambda_{in})V_L(\lambda_{out})} T_w(\bar{\lambda}) \times \exp\{-m[\tau_R(\lambda_{in}) + \tau_a(\lambda_{in}) - \tau_R(\lambda_{out}) - \tau_a(\lambda_{out})]\}. \quad (9)$$

Solving for $T_w(\bar{\lambda})$, we can relate this calculated value to the radiative transfer model calculation of $T_w(\bar{\lambda})$ to derive CWV. It is important to note that in Eq. (9) most measurements and calculated values appear as relative values, which we can determine more accurately than absolute values.^{24,32}

We applied method B to the IOP data obtained from the MFRSR and RSS instruments. For the MFRSR we used the 860- and 938-nm channels as λ_{out} and λ_{in} , respectively. $S(\lambda)$ of all the MFRSR channels was measured in August 1996 and again in March 1998. The 938-nm channel shifted toward red by 0.8 nm, but no wavelength shift was observed for the other channels. For the research reported in this paper we used the August 1996 measurements of $S(\lambda)$. For the RSS we used $\lambda_{out} = 871$ nm (pixel number 440) and $\lambda_{in} = 943$ nm (pixel number 458). The $S(\lambda)$ of each pixel was established by use of lasers.²¹ Because method B does not depend on modified Langley plots, no parameterization of $T_w(\bar{\lambda})$ is necessary, and $T_w(\bar{\lambda})$ can be converted into CWV from a look-up table. For both instruments we used MODTRAN 3.7 v1.0 to create such a look-up table of $T_w(\bar{\lambda})$ versus mu .

3. Method C: Empirical Technique

In method C the signal in the 938-nm MFRSR channel is calibrated for the retrieval of water vapor by estimation of the adjusted signal, $V_w(\lambda)$ (the signal that would be measured if water vapor were the only attenuator) with the MFRSR while the CWV is simultaneously observed with another instrument nearby. The other instrument is a microwave radiometer (MWR), the cloud and radiation test bed MWR (ARM CART), which measures at $f = 31.4$ and 23.8 GHz, which operates continuously at the SGP.³³ An empirical curve can then be formed that shows the relationship between $V_w(\lambda)$ and mu . An equation fitted to this curve provides an algebraic expression that relates $V_w(\lambda)$ and mu such that if $V_w(\lambda)$, the adjusted measurement, is known, then u can be found.

Using the definition of adjusted signal $V_w(\lambda)$ and Eq. (4), we have

$$V_w(\lambda) = V(\lambda) \exp\{m[\tau_R(\lambda) + \tau_a(\lambda) + \tau_3(\lambda)]\} = V_0(\lambda)d^{-2}T_w(\bar{\lambda}). \quad (10)$$

where $V(\lambda)$ is the measured voltage. $V_w(\lambda)$ is fitted by the four-parameter model:

$$V_w(\lambda)d^2 = V_0(\lambda) \exp[-a(mu)^{b-\beta mu}]. \quad (11)$$

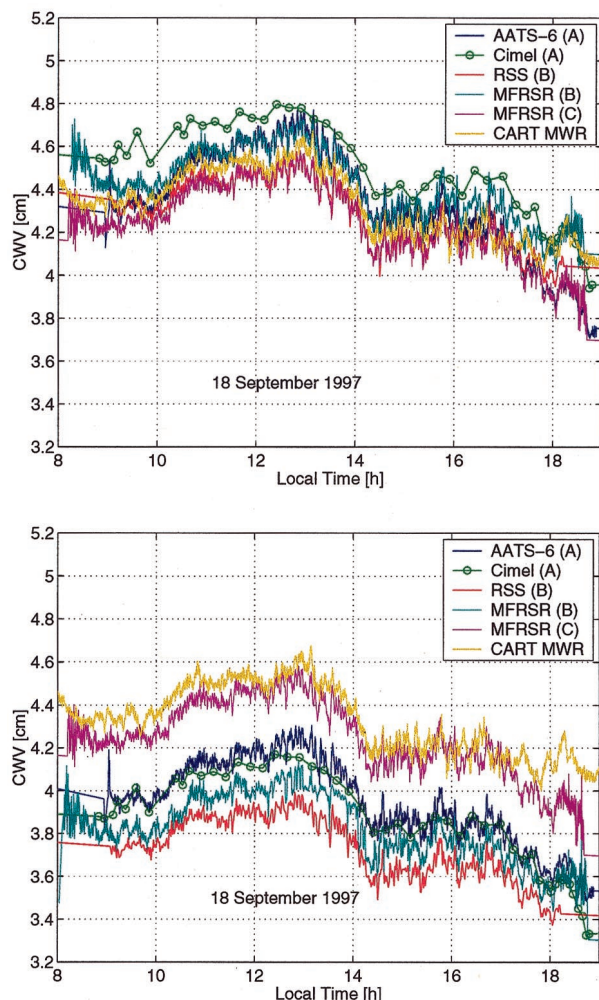


Fig. 1. Time series of columnar water vapor from different instruments and methods. Top, initial comparison for which no attempts have been made to standardize our procedure to one radiative transfer model. Bottom: All method A and method B retrievals use the same radiative transfer model (LBLRTM 5.10).

The four parameters are $V_0(\lambda)$, a , b , and β , where $V_0(\lambda)$ is the calibration constant for the 938-nm channel and a , b , and β describe $T_w(\bar{\lambda})$.

This form of $T_w(\bar{\lambda})$ is similar to the less-complicated transmission function in Eq. (6). We tried the simpler form, but it worked only over a small range of mu that is typical of dry conditions during the winter. To extend the applicability of the transmission function over a wider range of mu , encompassing the entire variation in vapor over the course of a year, we were forced to add a path dependence term, $-\beta mu$, to the exponent b , where β is a small correction term. With this addition the range of validity of Eq. (11) is $\sim 28 \text{ cm} \geq mu \geq 0 \text{ cm}$. We used data from 15 days of clear-sky conditions, spanning a period from 16 January to 28 August 1997, to determine $V_0(\lambda)$ and to develop the empirical transmission function described above. These data consisted of 21,278 20-s samples, and the parameter values were found to be $a = 0.5411$, $b = 0.5802$, and $\beta = 0.003284$, with u in units of precipitable centimeters.

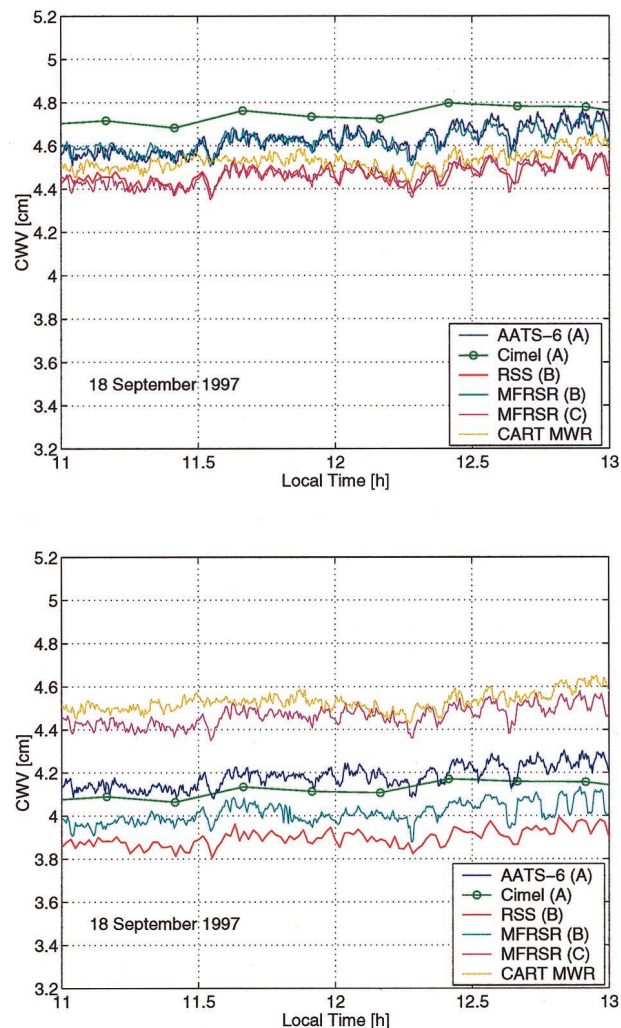


Fig. 2. Same as Fig. 1, but only two hours are shown to show small-scale variations better.

In method C the need to calibrate with the modified Langley method and the use of a radiative transfer model are both avoided. However, we have to keep in mind that, because the parameters in Eq. (11) are determined by comparison with the MWR, method C cannot yield an independent measurement of CWV.

4. Results

In the first round, as with the AOD intercomparison,¹⁷ we made no attempt to standardize our procedures to the use of the same radiative transfer model and its underlying water-vapor spectroscopy (required for methods A and B). In the second round we used the line-by-line radiative transfer model LBLRTM 5.10 (Ref. 34) for all method A and method B retrievals. As with the AOD intercomparison,¹⁷ we compared all the CWV retrievals with the AATS-6 results. Because of the different sampling strategies and days of operation, we obtained as few as 466 to as many as $\sim 19,000$ samples in the comparisons. The results were analyzed in terms of time series (Figs. 1 and 2) and scatterplots (Figs. 3 and 4). Sta-

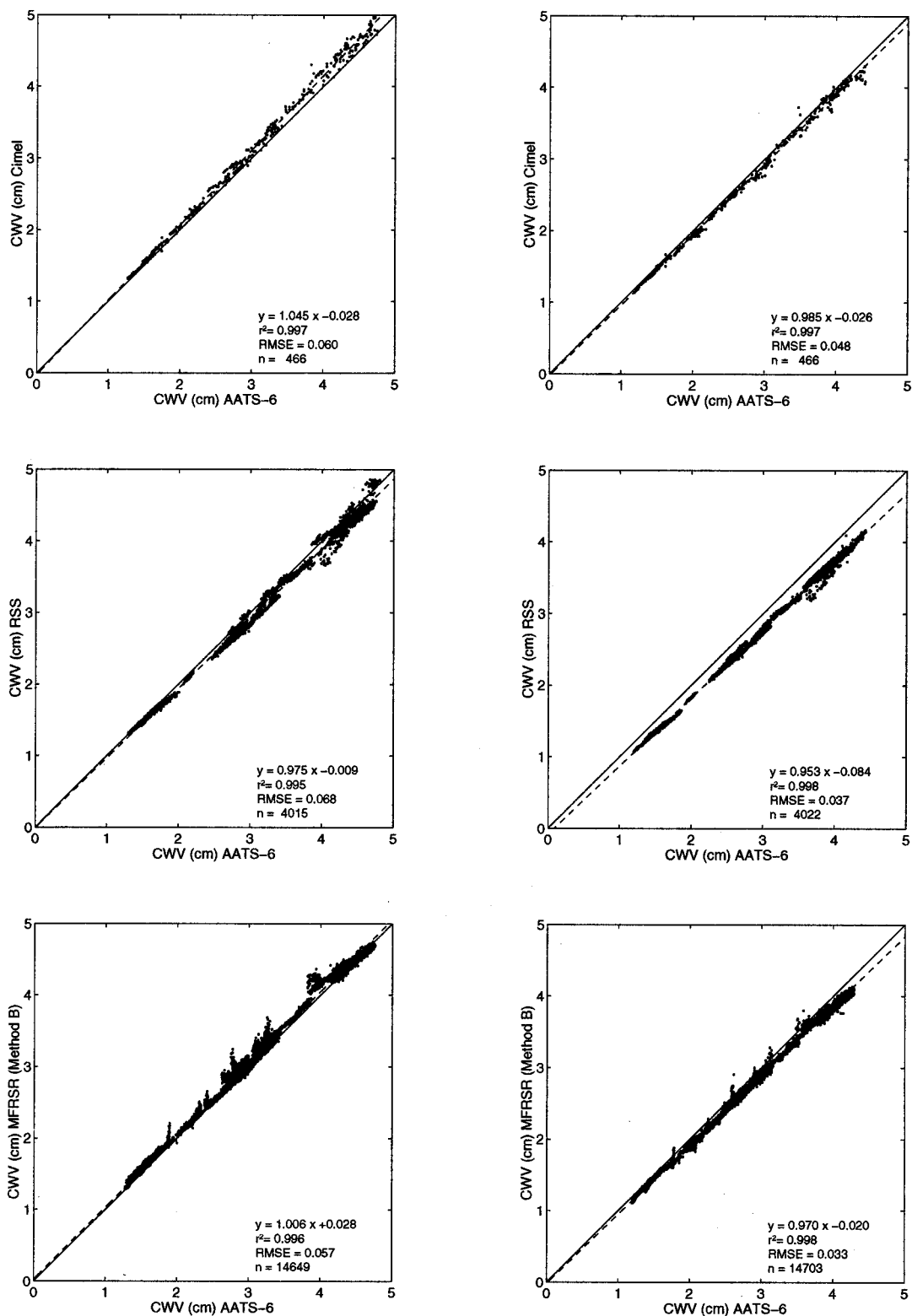


Fig. 3. CWV comparison with the AATS-6. Left, initial comparison, for which no attempts have been made to standardize our procedure to one radiative transfer model. Right, retrievals were made with the same radiative transfer model (LBLRTM 5.10). rmse, root mean square error with respect to the best-fit line.

tistical summaries are given in tabular form in Tables 2 and 3 and are illustrated in Fig. 5.

We found that the quality of the MFRSR retrievals (Methods B and C) deteriorates at larger slant-path

water-vapor amounts μ , prompting us to use MFRSR data with $\mu < 23$ cm. The Cimel and AATS-6 retrievals do not have that limitation, and no RSS retrievals were available for large values of μ .

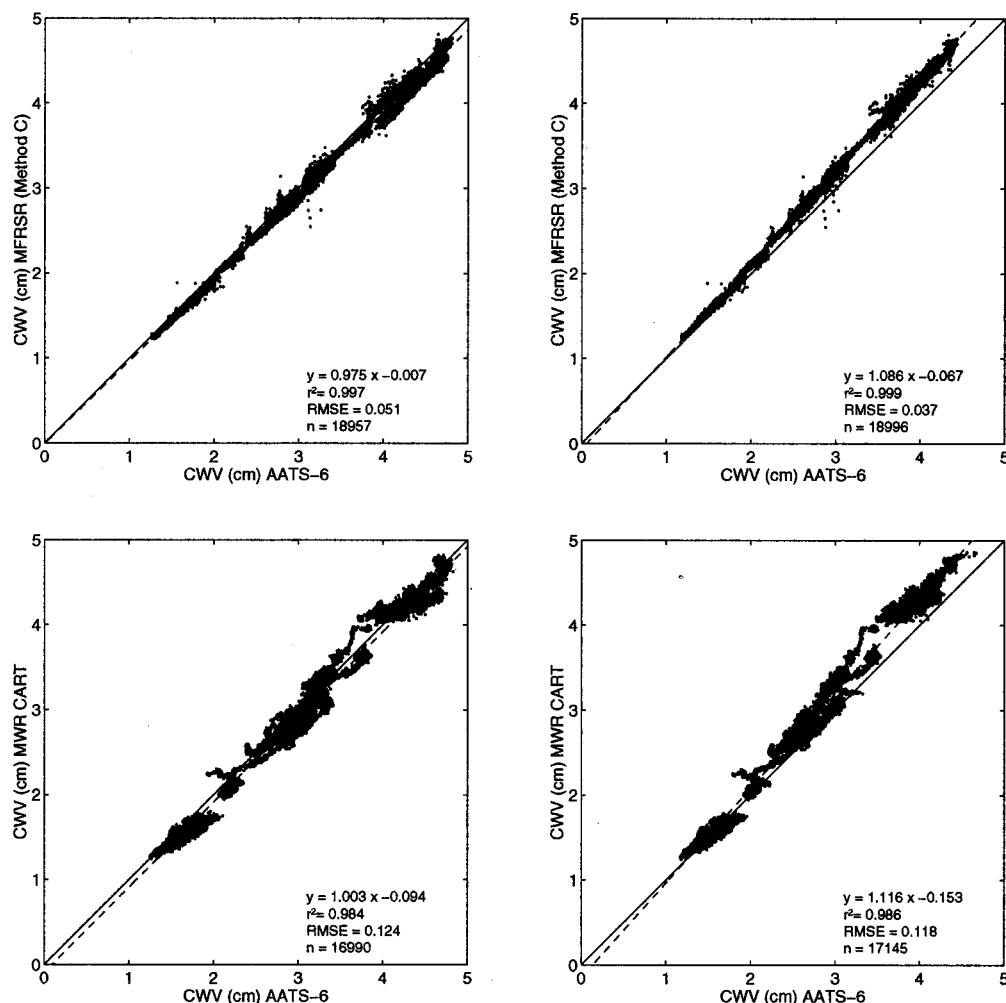


Fig. 4. CWV comparison with the AATS-6. Left, initial comparison, for which MODTRAN 3.5 was used for the AATS-6. Right, LBLRTM 5.10 was used for the AATS-6.

The scatterplots (Figs. 3 and 4) reveal a high correlation ($0.995 \leq r^2 \leq 0.999$) among the solar transmittance methods and a somewhat smaller correlation ($0.984 \leq r^2 \leq 0.986$) with the MWR. This is so because the MWR and the optical instruments, despite their collocation, did not observe the same volume of air because the viewing direction is zenith for the MWR and slant-path-to-Sun for the

solar radiometers; furthermore, the FOV's of the MWR [4.5° and 5.9° (FWHM) at 31.4 and 23.8 GHz, respectively] are larger. Consequently we observe from Fig. 2 that the small-scale variations in CWV are highly correlated among the solar radiometers, whereas some of the small-scale features are absent from the MWR data. Also, we have generally found that the correspondence between solar and micro-

Table 2. Comparison of CWV from Various Instruments and Methods with the AATS-6 Instrument^a

| Instrument | Method | Model | n | Best Fit | | | Mean (cm) | | Difference (cm) | | | Ratio y/AATS-6 | | |
|------------|--------------|--------------|-------|----------|----------------|----------------|-----------|----------|-----------------|--------------------|------|----------------|------|--------------------|
| | | | | Slope | Intercept (cm) | r ² | rms (cm) | AATS-6 y | Mean | Standard Deviation | rms | % rms | Mean | Standard Deviation |
| AATS-6 | A | MODTRAN 3.5 | | | | | | | | | | | | |
| Cimel | A | LOWTRAN 7 | 466 | 1.05 | -0.03 | 0.997 | 0.06 | 2.83 | 2.93 | 0.10 | 0.08 | 0.13 | 4.4 | 1.03 |
| RSS | B | MODTRAN 3.7 | 4015 | 0.98 | -0.01 | 0.995 | 0.07 | 3.06 | 2.98 | -0.09 | 0.07 | 0.11 | 3.7 | 0.97 |
| MFRSR | B | MODTRAN 3.7 | 14649 | 1.01 | 0.03 | 0.996 | 0.06 | 2.73 | 2.77 | 0.04 | 0.06 | 0.07 | 2.6 | 1.02 |
| MFRSR | C | ^b | 18957 | 0.98 | -0.01 | 0.997 | 0.05 | 2.86 | 2.78 | -0.08 | 0.06 | 0.10 | 3.4 | 0.97 |
| MWR CART | ^b | ^b | 16990 | 1.00 | -0.09 | 0.984 | 0.12 | 2.87 | 2.79 | -0.09 | 0.12 | 0.15 | 5.3 | 0.97 |

^aThis is the initial comparison, in which different radiative transfer models as indicated were used.

^bNot applicable.

Table 3. Same as Table 2 but with the Same Radiative Transfer Model Used for All Method A and Method B Retrievals

| Instrument | Method | Model | n | Best Fit | | | Mean (cm) | | Difference (cm) | | | Ratio y/AATS-6 | | |
|------------|--------------|--------------|-------|----------|----------------|-------|-----------|--------|-----------------|-------|--------------------|----------------|-----|--------------------|
| | | | | Slope | Intercept (cm) | r^2 | rms (cm) | AATS-6 | y | Mean | Standard Deviation | rms | % | Standard Deviation |
| | | | | | | | | | | | | | | |
| AATS-6 | A | LBLRTM 5.10 | | | | | | | | | | | | |
| Cimel | A | LBLRTM 5.10 | 466 | 0.99 | -0.03 | 0.997 | 0.05 | 2.60 | 2.54 | -0.06 | 0.05 | 0.08 | 3.2 | 0.97 |
| RSS | B | LBLRTM 5.10 | 4022 | 0.95 | -0.08 | 0.998 | 0.04 | 2.80 | 2.59 | -0.22 | 0.06 | 0.22 | 8.0 | 0.92 |
| MFRSR | B | LBLRTM 5.10 | 14703 | 0.97 | -0.02 | 0.998 | 0.03 | 2.50 | 2.41 | -0.10 | 0.04 | 0.10 | 4.1 | 0.96 |
| MFRSR | C | ^a | 18996 | 1.09 | -0.07 | 0.999 | 0.04 | 2.63 | 2.78 | 0.16 | 0.09 | 0.18 | 6.9 | 1.06 |
| MWR CART | ^a | ^a | 17145 | 1.12 | -0.15 | 0.986 | 0.12 | 2.64 | 2.79 | 0.15 | 0.16 | 0.22 | 8.3 | 1.05 |

^aNot applicable.

wave radiometers is best near solar noon. In the first round of comparison three different models were used for the method A and method B retrievals. The results are shown at the left in Figs. 3 and 4 and are summarized in Table 2 and Fig. 5. The differences between each method (including that of the MWR) and the AATS-6 range from 2.6% to 5.3% (rms). The mean differences are within ± 0.1 cm, and the mean ratios range from 0.97 to 1.03.

In the second round of comparison we used the LBLRTM 5.10 model (which includes the updated spec-

troscopy of Giver *et al.*¹²) for all method A and method B retrievals. Repeating the computation with the LBLRTM 5.21 model (the most recent version at the time of writing) led to identical results. In this second round we also deviated from the standard Cimel AERONET CWV algorithm (which uses a typical 940-nm filter function for all instruments) by using the measured filter functions for instruments #27 and #37. The results are shown at the right in Figs. 3 and 4 as scatterplots and are summarized in Table 3 and Fig. 5.

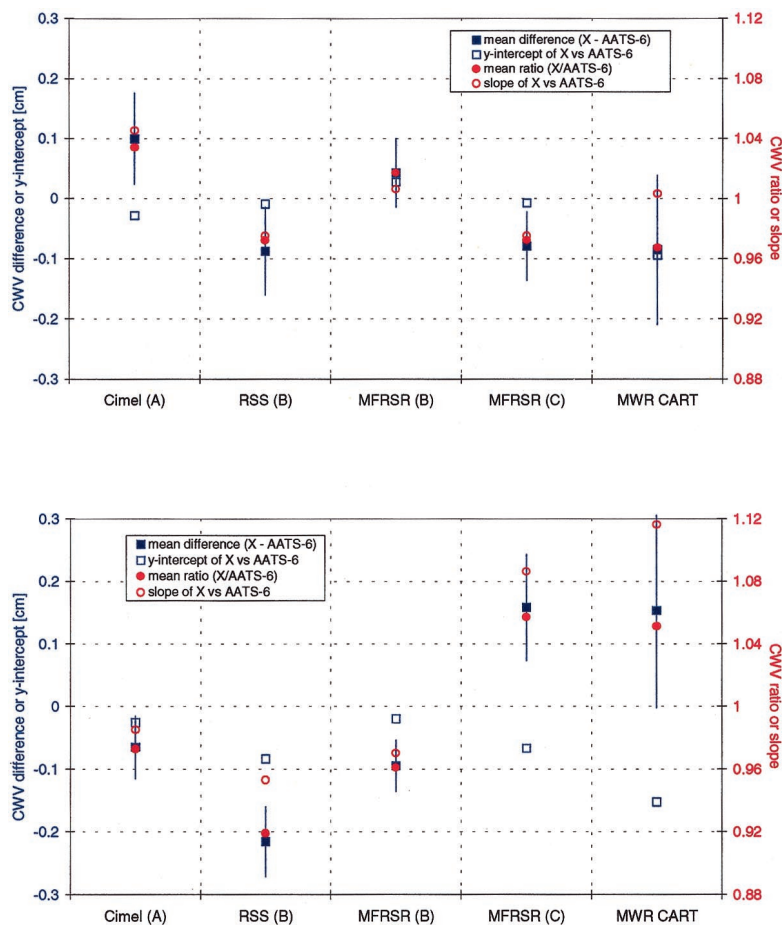


Fig. 5. Statistics for CWV comparison with the AATS-6. Top, initial comparison, for which no attempts have been made to standardize our procedure to one radiative transfer model. Bottom, all method A and method B retrievals used the same radiative transfer model (LBLRTM 5.10).

As can be seen from the time series in Figs. 1 and 2, the changes made in the second comparison had a significant effect. Overall they decreased the mean CWV by 8% for the AATS-6 and by 13% for the Cimel, RSS, and MFRSR instruments (method B). These decreases in CWV are consistent with the results reported by Ingold *et al.*³ Although we observe an even better correlation among the different methods (r^2 closer to unity and smaller rms differences with respect to the best-fit line), we now find larger biases. The differences of the results of each method (including that of the MWR) from those of the AATS-6 now range from 3.2% to 8.3% (rms). The mean absolute differences in the CWV range from -0.22 to 0.16 cm, with mean ratios from 0.92 to 1.06 . The results of methods A and B are now 6–14% lower than the results of the MWR, and, consequently, of method C. Compared with the AATS-6, the MWR and the MFRSR (method C) exhibit slopes that deviate considerably from unity. Note that the MFRSR (method C) retrievals are tied to MWR results.

Even the spread among the results of the independent solar transmittance retrievals (methods A and B) has increased slightly. In terms of absolute differences the spread (difference between the largest and the smallest values in columns 11 of Tables 2 and 3) is now 0.22 cm (previously 0.19 cm), or, in terms of mean ratios (difference between largest and smallest values in columns 15 of Tables 2 and 3) the spread increased from 6% to 8%. This finding shows that the result of the first comparison round was somewhat misleading because differences in the models obviously compensated for other existing biases. In other words, the remaining biases must be caused by errors other than model errors. For method A, these errors include uncertainty primarily in the calibration constant $V_0(\lambda)$, in the filter function $S(\lambda)$, in the parameterization of T_w , and in the aerosol optical depth $\tau_a(\lambda)$. A detailed analysis of these uncertainties can be found in Ref. 3. For method B, uncertainties other than model errors include uncertainty in the filter function $S(\lambda)$, the lamp irradiance ratio $E_L(\lambda_{in})/E_L(\lambda_{out})$, the relative extraterrestrial solar spectrum ratio $E_0(\lambda_{in})/E_0(\lambda_{out})$, and $\tau_a(\lambda)$. A detailed discussion of these uncertainties is given by Michalsky *et al.*³¹ Here we have used the extraterrestrial solar spectrum compiled by Gueymard³⁵ for the method B retrievals. Using the spectrum of Kuzucz³⁶ as contained in MODTRAN 3.7 increased the mean CWV by 1.3%.

5. Conclusions

We have in hand a large data set of CWV retrievals from four solar radiometers. We used three different retrieval techniques and also compared them with a MWR, on which one of the techniques is based. The good agreement realized in the first round of comparison turns out to be fortuitous because differences in the radiative transfer models obviously compensated for biases found once a single model was used for all independent retrievals. The spread of 0.22 cm, or 8%, among all indepen-

dent solar radiometer retrievals when the same model was used is an indication of the other-than-model uncertainties involved in determining CWV from solar transmittance measurements with current instrumentation. These uncertainties include primarily uncertainties in calibration and filter or slit-function profile.

The changes in H_2O spectroscopy suggested by Giver *et al.*¹² (a 14.4% increase of the line strengths for the $0.94\text{-}\mu\text{m}$ band) had a significant effect on the retrievals: Depending on which model was used initially, the changes decreased the mean CWV by 8% or 13%. With the newer spectroscopy the CWV retrievals from the solar radiometers are now 6–14% lower than for the MWR results. However, this result needs to be considered in context with all CWV measurements performed during the IOP (a publication showing all results from the second water vapor IOP is in preparation). Furthermore, a recent study by Belmiloud *et al.*³⁷ suggests that there is an additional 6% increase in the strength of the $0.94\text{-}\mu\text{m}$ water-vapor absorption band.

Appendix A: Authors' Affiliations

B. Schmid (bschmid@mail.arc.nasa.gov) is with the Bay Area Environmental Research Institute, 3430 Noriega Street, San Francisco, California 94122. J. J. Michalsky (joe@asrc.cestm.Albany.edu) is with the Atmospheric Sciences Research Center, State University of New York, Albany, 251 Fuller Road, Albany, New York 12203. D. W. Slater (donald.slater@pnl.gov) and J. C. Barnard (james.barnard@pnl.gov) are with the Pacific Northwest National Laboratory, P.O. Box 999, Richland, Washington 99352. R. N. Halthore (halthore@poamc.nrl.navy.mil) is with the U.S. Naval Research Laboratory, Code 7228, 4555 Overlook Avenue, S.W., Washington, D.C. 20375. When this research was performed, R. N. Halthore was with the Brookhaven National Laboratory, Upton, New York 11973-5000. J. C. Liljegren (jcliljegren@anl.gov) is with the Argonne National Laboratory, 9700 South Cass Avenue, Argonne, Illinois 60439. When this research was performed, J. C. Liljegren was with the Ames Laboratory, Ames, Iowa 50011. B. N. Holben (brent@aeronet.gsfc.nasa.gov) is with the NASA Goddard Space Flight Center, Code 923, Greenbelt, Maryland 20771. T. F. Eck (tom@aeronet.gsfc.nasa.gov) is with Raytheon Information Technology and Scientific Services, NASA Goddard Space Flight Center, Code 923, Greenbelt, Maryland 20771. J. M. Livingston (jlivingston@mail.arc.nasa.gov) is with SRI International, 333 Ravenswood Avenue, Menlo Park, California 94025. P. B. Russell (prussell@mail.arc.nasa.gov) is with NASA Ames Research Center, MS 245-5, Moffett Field, California 94035-1000. T. Ingold (ingold@mw.iap.unibe.ch) is with the Institute of Applied Physics, University of Bern, Sidlerstrasse 5, CH-3012 Bern, Switzerland. I. Slutsker (ilya@aeronet.gsfc.nasa.gov) is with Science Systems and Applications, Inc., NASA Goddard

Space Flight Center, Code 923, Greenbelt, Maryland 20771.

The Office of Earth Science, NASA Headquarters (Robert Curran and Jack Kaye) and the National Oceanic and Atmospheric Administration Office of Global Programs (Joel Levy) funded this research in part (grants to Bay Area Environmental Research Institute, SRI International, and NASA Ames Laboratory). The research was also supported by the Office of Biological and Environmental Research of the U.S. Department of Energy as part of the Atmospheric Radiation Measurement Program through grant DE-FG02-90ER61072 (State University of New York) and by contract DE-AC02-98CH10886 (Brookhaven National Laboratory), and contracts CHENG82-1010502-0002884 (Ames Laboratory) and W-31-109-Eng-38 (Argonne National Laboratory). The Pacific Northwest National Laboratory is operated for the U.S. Department of Energy by Battelle Memorial Institute under contract DE-AC0676RLO 1830. The AERONET project is supported by the Earth-Observing System Project Science Office (Michael King) and the Office of Earth Science, NASA Headquarters (Robert Curran).

References

1. R. M. Goody and Y. L. Yung, *Atmospheric Radiation: Theoretical Basis*, 2nd ed. (Oxford U. Press, Oxford, 1989).
2. F. E. Fowle, "The spectroscopic determination of aqueous vapor," *Astrophys. J.* **35**, 149–162 (1912).
3. T. Ingold, B. Schmid, C. Mätzler, P. Demoulin, and N. Kämpfer, "Modeled and empirical approaches for retrieving columnar water vapor from solar transmittance measurements in the 0.72, 0.82 and 0.94- μm absorption bands," *J. Geophys. Res.* **105**, 24,327–24,343 (2000).
4. B. Schmid, J. M. Livingston, P. B. Russell, P. A. Durkee, H. H. Jonsson, D. R. Collins, R. C. Flagan, J. H. Seinfeld, S. Gassó, D. A. Hegg, E. Öström, K. J. Noone, E. J. Welton, K. J. Voss, H. R. Gordon, P. Formenti, and M. O. Andreae, "Clear sky closure studies of lower tropospheric aerosol and water vapor during ACE 2 using airborne sunphotometer, airborne in-situ, space-borne, and ground-based measurements," *Tellus B* **52**, 568–593 (2000).
5. W. P. Chu, E. W. Chiou, J. C. Larsen, L. W. Thomason, D. Rind, J. J. Buglia, S. Oltmans, M. P. McCormick, and L. M. McMaster, "Algorithms and sensitivity analyses for Stratospheric Aerosol and Gas Experiment. II. Water vapor retrieval," *J. Geophys. Res.* **98**, 4857–4866 (1993).
6. J. D. Lumpe, R. M. Bevilacqua, K. W. Hoppel, S. S. Krigman, D. L. Kriebel, C. E. Randall, D. W. Rusch, C. Brogniez, R. Ramanananaherosa, E. P. Shettle, J. J. Olivero, J. Lenoble, and P. Pruvost, "POAM II retrieval algorithm and error analysis," *J. Geophys. Res.* **102**, 23,593–23,614 (1997).
7. B.-C. Gao and A. F. H. Goetz, "Column atmospheric water vapor and vegetation liquid water retrievals from airborne imaging spectrometer data," *J. Geophys. Res.* **95**, 3549–3564 (1990).
8. Y. J. Kaufman and B.-C. Gao, "Remote sensing of water vapor in the near IR from EOS/MODIS," *IEEE Trans. Geosci. Remote Sens.* **30**, 871–884 (1992).
9. S. Bouffiès, F. M. Bréon, D. Tanré, and P. Dubuisson, "Atmospheric water vapor estimate by a differential absorption technique with the polarisation and directionality of the Earth reflectances (POLDER) instrument," *J. Geophys. Res.* **102**, 3831–3841 (1997).
10. M. Vesperini, F. M. Bréon, and D. Tanré, "Atmospheric water vapor content from spaceborne POLDER measurements," *IEEE Trans. Geosci. Remote Sens.* **37**, 1613–1619 (1999).
11. L. S. Rothman, C. P. Rinsland, A. Goldman, S. T. Massie, D. P. Edwards, J.-M. Flaud, A. Perrin, C. Camy-Peyret, V. Dana, J.-Y. Mandin, J. Schroeder, A. McCann, R. R. Gamache, R. B. Wattson, K. Yoshino, K. V. Chance, K. W. Jucks, L. R. Brown, V. Nemtchinov, and P. Varanasi, "The HITRAN molecular spectroscopic database and HAWKS (HITRAN atmospheric workstation): 1996 edition," *J. Quant. Spectrosc. Rad. Transfer* **60**, 665–710 (1998).
12. L. P. Giver, C. Chackerian, Jr., and P. Varanasi, "Visible and near-infrared H_2^{16}O line intensity corrections for HITRAN-96," *J. Quant. Spectrosc. Rad. Transfer* **66**, 101–105 (2000).
13. R. C. M. Learner, W. Zhong, J. D. Haigh, D. Belmiloud, and J. Clarke, "The contribution of unknown weak water vapor lines to the absorption of solar radiation," *Geophys. Res. Lett.* **26**, 3609–3612 (1999).
14. M. Carleer, A. Jenouvrier, A.-C. Vandaele, P. F. Bernath, M. F. Mérianne, R. Colin, N. F. Zobov, O. L. Polyansky, J. Tennyson, and V. A. Savin, "The near infrared, visible, and near ultraviolet overtone spectrum of water," *J. Chem. Phys.* **111**, 2444–2450 (1999).
15. G. M. Stokes and S. E. Schwartz, "The atmospheric radiation measurement (ARM) program: programmatic background and design of the cloud and radiation test bed," *Bull. Am. Meteorol. Soc.* **75**, 1201–1221 (1994).
16. H. E. Revercomb, W. F. Feltz, R. O. Knuteson, D. C. Tobin, P. F. W. van Delst, and B. A. Whitney, "Accomplishments of the water vapor IOPs: an overview," presented at the Eighth Atmospheric Radiation Measurement (ARM) Science Team Meeting, 23–27 March 1998, Tucson, Ariz.).
17. B. Schmid, J. Michalsky, R. Halthore, M. Beauharnois, L. Harrison, J. Livingston, P. Russell, B. Holben, T. Eck, and A. Smirnov, "Comparison of aerosol optical depth from four solar radiometers during the Fall 1997 ARM intensive observation period," *Geophys. Res. Lett.* **26**, 2725–2728 (1999).
18. T. Matsumoto, P. B. Russell, C. Mina, W. Van Ark, and V. Banta, "Airborne tracking sunphotometer," *J. Atmos. Ocean. Technol.* **4**, 336–339 (1987).
19. B. N. Holben, T. F. Eck, I. Slutsker, D. Tanré, J. P. Buis, A. Setzer, E. Vermote, J. A. Reagan, Y. J. Kaufman, T. Nakajima, F. Lavenu, I. Jankowiak, and A. Smirnov, "AERONET: a federated instrument network and data archive for aerosol characterization," *Remote Sens. Environ.* **66**, 1–16 (1998).
20. L. Harrison, J. Michalsky, and J. Berndt, "Automated multi-filter rotating shadow-band radiometer: an instrument for optical depth and radiation measurements," *Appl. Opt.* **33**, 5118–5125 (1994).
21. L. Harrison, M. Beauharnois, J. Berndt, P. Kiedron, J. J. Michalsky, and Q. Min, "The rotating shadowband spectroradiometer (RSS) at SGP," *Geophys. Res. Lett.* **26**, 1715–1718 (1999).
22. F. Kasten and A. T. Young, "Revised optical air mass tables and approximation formula," *Appl. Opt.* **28**, 4735–4738 (1989).
23. B. Schmid and C. Wehrli, "Comparison of sun photometer calibration by use of the Langley technique and the standard lamp," *Appl. Opt.* **34**, 4500–4512 (1995).
24. B. Schmid, P. R. Spyak, S. F. Biggar, C. Wehrli, J. Sekler, T. Ingold, C. Mätzler, and N. Kämpfer, "Evaluation of the applicability of solar and lamp radiometric calibrations of a precision Sun photometer operating between 300 and 1025 nm," *Appl. Opt.* **37**, 3923–3941 (1998).
25. P. B. Russell, J. M. Livingston, E. G. Dutton, R. F. Puschel, J. A. Reagan, T. E. Defoor, M. A. Box, D. Allen, P. Pilewski, B. M. Herman, S. A. Kinne, and D. J. Hofmann, "Pinatubo and pre-Pinatubo optical-depth spectra: Mauna Loa measurements, comparisons, inferred particle size distributions, radi-

- ative effects, and relationship to lidar data," *J. Geophys. Res.* **98**, 22,969–22,985 (1993).
26. J. A. Reagan, P. A. Pilewskie, I. C. Scott-Fleming, B. M. Herman, and A. Ben-David, "Extrapolation of Earth-based solar irradiance measurements to exoatmospheric levels for broadband and selected absorption-band observations," *IEEE Geosci. Rem. Sens.* **25**, 647–653 (1987).
 27. J. J. Michalsky, J. C. Liljegren, and L. C. Harrison, "A comparison of Sun photometer derivations of total column water vapor and ozone to standard measures of same at the Southern Great Plains Atmospheric Radiation Measurement site," *J. Geophys. Res.* **100**, 25,995–26,003 (1995).
 28. B. Schmid, K. J. Thome, P. Demoulin, R. Peter, C. Mätzler, and J. Sekler, "Comparison of modeled and empirical approaches for retrieving columnar water vapor from solar transmittance measurements in the 0.94 micron region," *J. Geophys. Res.* **101**, 9345–9358 (1996).
 29. R. N. Halthore, T. F. Eck, B. N. Holben, and B. L. Markham, "Sun photometric measurements of atmospheric water vapor column abundance in the 940-nm band," *J. Geophys. Res.* **102**, 4343–4352 (1997).
 30. F. X. Kneizys, L. W. Abreu, G. P. Anderson, J. H. Chetwynd, E. P. Shettle, A. Berk, L. S. Bernstein, D. C. Robertson, P. Acharaya, L. S. Rothmann, J. E. A. Selby, W. O. Gallery, and S. A. Clough, "The Modtran 2/3 report and LOWTRAN 7 model," (Phillips Laboratory, Hanscom Air Force Base, Mass., 1996).
 31. J. J. Michalsky, Q. Min, P. W. Kiedron, D. W. Slater, and J. C. Barnard, "A differential technique to retrieve column water vapor using sun radiometry," *J. Geophys. Res.* (to be published).
 32. P. W. Kiedron, J. J. Michalsky, J. L. Berndt, and L. C. Harrison, "Comparison of spectral irradiance standards used to calibrate shortwave radiometers and spectroradiometers," *Appl. Opt.* **38**, 2432–2439 (1999).
 33. J. C. Liljegren, "Automatic self-calibration of ARM microwave radiometers," in *Microwave Radiometry and Remote Sensing of the Earth's Surface and Atmosphere*, P. Pampaloni and S. Paloscia, eds., (VSP Press, Utrecht, The Netherlands, 1999).
 34. S. A. Clough and M. J. Iacono, "Line-by-line calculations of atmospheric fluxes and cooling rates. II. Application to carbon dioxide, ozone, methane, nitrous oxide, and the halocarbons," *J. Geophys. Res.* **100**, 16,519–16,535 (1995).
 35. C. Gueymard, "SMARTS2, a simple model of the atmospheric radiative transfer of sunshine: algorithms and performance assessment," Rep. FSEC-PF-270-95 (Florida Solar Energy Center, Cocoa, Fla., 1995).
 36. R. L. Kurucz, "The solar irradiance by computation," in *Proceedings of the 17th Annual Conference on Atmospheric Transmission Models*, G. P. Anderson, R. H. Picard, and J. H. Chetwynd, eds., Rep. PL-TR 95 2060 (U.S. Air Force Geophysics Laboratory, Hanscom Air Force Base, Mass., 1994), pp. 333–334.
 37. D. Belmiloud, R. Schermaul, K. M. Smith, N. F. Zobov, J. W. Brault, R. C. M. Learner, D. A. Newnham, and J. Tennyson, "New studies of the visible and near-infrared absorption by water vapour and some problems with the HITRAN database," *Geophys. Res. Lett.* **27**, 22, 3703–3706 (2000).